Dynamic modeling and model-based control of a twin screw extruder

Jonathan Grimard, Laurent Dewasme and Alain Vande Wouwer

***Abstract*— Hot-melt extrusion is a popular process in the field of industrial product manufacturing. In this work, a simple distributed parameter model consisting in partial differential equations derived from mass balances, well-adapted to the design of a control strategy, is expressed. Parameter identification is applied to a specific device with a complex screw geometry and provides a good representation of the extruder behavior. Due to the existence of strong nonlinearities and complex input-output coupling, a nonlinear model predictive control (NMPC) strategy is proposed and designed to regulate the output active pharmaceutical ingredient (API) concentration and the output flow. The effectiveness of this strategy is demonstrated by numerical validations and robustness analysis with respect to measurement noise and model uncertainties.**

I. Introduction

The hot-melt extrusion process is a well-established forming method which consists in conveying (thanks to the screw rotation) several solid materials through the extruder so as to transform them into a specific uniform product [1]. The increasing popularity of hot melt extrusion leads to numerous extruded products: metals, plastics, foods, drugs ... In the pharmaceutical context, an active pharmaceutical ingredient (API) is generally mixed and heated with a thermoplastic polymer and different excipients (surfactants, salts, super disintegrants, plasticizers and antioxidants) are added to obtain desired final product properties [2]. The product quality is impacted by several physical parameters such as the barrel temperature, the screw configuration, the rotation speed and the feed rate [3]. Analysis of these factors can therefore be performed to optimize the process performance while complying with stringent manufacturing constraints.

Along with the desired properties of the final products, other constraints such as the energy savings, process performance and operating cost reduction are increasingly imposed to industrial devices. However the application of control strategies to extrusion processes are relatively rare in the literature. Most of the proposed strategies are based on modeling the system by simple transfer functions, and range from PID control ([4],[5],[6]) to model predictive control ([7],[8]). Application of a fuzzy control has also been proposed and is studied in [9]. The full predictive capability of a first-principle partial differential equation model within a model-based control is another interesting approach which is the main motivation of this study.

In this work, the regulation of an extrusion process dedicated to manufacturing of pharmaceutical tablets is considered. Several mechanisms involved in the mixing between a polymeric matrix and an active pharmaceutical ingredient (API) are described using a dynamic distributed parameter model inspired from previous works ([10], [11]) in section II. Fitting with measurements of the residence time distribution (RTD) enables the identification of several transportation parameters in section III. Section IV studies the application of Non Linear Model Predictive Control (NMPC). Conclusions are drawn in section V.

[1]Service d'Automatique, Université de Mons, Bd. Dolez 31, 7000 Mons - Belgique jonathan.grimard@umons.ac.be, laurent.dewasme@umons.ac.be, alain.vandewouwer@umons.ac.be

II. Extruder dynamic modeling

In this section, the derivation of an appropriate dynamic model for the design and the implementation of a control strategy is presented. In [11], a complex dynamic model composed of partial derivative equations based on mass and energy balances has been proposed, providing satisfactory prediction. Unfortunately, the numerical simulation of this model requiers high computational efforts which makes this model inappropriate for on-line control.

Some simplifications of this previous model are therefore suggested. The internal configuration of the extrusion device is composed of one partially filled zone to represent the transportation of the material and one completely filled zone to describe process mixing effects (see Figure 1). Four inputs are considered : the feed flow rate Q_{in}, the screw rotation speed N, the inlet active product concentration C_{in} and the barrel temperature T_b; while the filling ratio f, the pressure P, the output mass flow Q^{out} and the output API concentration C^{out} form the system outputs.

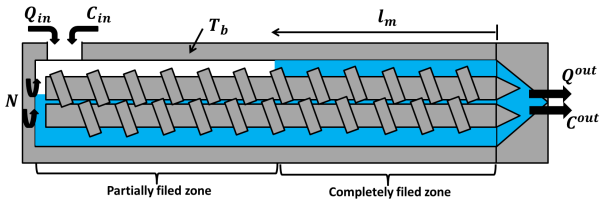

Fig. 1. Configuration and variables of the model

Only mass balances are expressed while modeling the partially and completely filled zones. Energy balances are indeed not used and material temperature is considered equal to the barrel temperature T_b (heat transfers inside the barrel are assumed to be perfect).

A. Mass balances

1) Partially Filled Zone: The device inlet is composed of a conveying zone, which is partially filled (filling ratio f

is smaller than 1). Two kinds of flow rates characterize the transport of the material: a convective flow, which is related to the screw rotation, and a diffusive flow. Evolution of the filling ratio can therefore be defined by the following mass balance equation:

$$\frac{\partial f}{\partial t} = -\frac{V_c N}{S}\frac{\partial f}{\partial z} + D\frac{\partial^2 f}{\partial z^2} \tag{1}$$

where ρ, S, N are respectively the material density, the cross section area for material transportation and the screw rotation speed. V_c is the shear volume and D is the dispersion coefficient, which are considered as unknown.

2) Completely Filled Zone: Mass accumulation is observed at the device outlet due to the die shape. Therefore, the filling ratio f is equal to 1 and imposes the existence of a counter-current flow. Following [12], this flow obeys the Poiseuille theory and is driven by a pressure difference. Moreover, the total mass flow Q_m is conserved inside the completely filled zone and is given by:

$$Q_m = \rho V_c N - \rho\frac{K_r}{\eta}\frac{\partial P}{\partial z} \tag{2}$$

where K_r is an unknown geometrical coefficient and P the pressure.

From equation 2, the pressure gradient can be determined:

$$\frac{\partial P}{\partial z} = \frac{(V_c N - \frac{Q_m}{\rho})}{K_r}\eta(z) \tag{3}$$

Output mass flow Q^{out} is calculated considering, as in [13], that the extruder output is comparable to a tube in which a Poiseuille flow takes place:

$$Q^{out} = \rho K_f (P_{end} - P_0) \tag{4}$$

where P_{end} is the output pressure and K_f is the output geometrical constant obtained as:

$$K_f = \frac{\pi {R_f}^4}{8 L_f \eta_{end}} \tag{5}$$

where R_f is the output radius, L_f its length and η_{end} the output material dynamic viscosity.

B. Active pharmaceutical ingredient concentration

Several elements compose the conveying material assumed to be a matrix in which an active product is simply inserted without any chemical reaction. Mass balance taking convective and diffusive flows into account enables the determination of the active pharmaceutical ingredient concentration C evolution as follows:

$$f\frac{\partial C}{\partial t} = -\frac{Q}{\rho S}\frac{\partial C}{\partial z} + D\frac{\partial^2 C}{\partial z^2} \tag{6}$$

C. Moving interface equation:

The evolution of the completely filled zone length l_m must be calculated since it allows to take important influences of the barrel temperature T_b and the screw rotation N on the system into account. In this study, the approach of [10] is selected, where this evolution is formulated through a mass balance based on the calculation of the material quantity partially filling the zone.

$$S(1 - f_{pc})\rho\frac{\partial l_m}{\partial t} = Q_{pc} - Q_m \tag{7}$$

where f_{pc} is the boundary filling ratio, l_m the melting zone length and Q_{pc} the boundary mass flow.

The completely filled zone length is therefore calculated by the following equation:

$$\frac{\partial l_m}{\partial t} = \frac{Q_{pc} - Q_m}{S(1 - f_{pc})\rho} \tag{8}$$

D. Dynamic viscosity evolution

Rheological properties of the material must also be modeled since these characteristics have significant influences on the mass flows. Therefore, variations of the dynamic viscosity η along the extruder screws are represented while the density is assumed to be constant. A nonlinear function is selected and, as in [13] and [14], the Yasuda-Carreau law is chosen. The expression is formulated as:

$$\eta = \eta_0(t)[1 + (\lambda_t\dot{\gamma})^a]^{\frac{(n-1)}{a}} \tag{9}$$

where $\eta_0(t)$ is the zero shear viscosity, λ_t the characteristic matrix time constant, $\dot{\gamma}$ the shear rate, a the Yasuda parameter and n the pseudo-plastic index. These different parameters are determined with respect to the material properties which are assumed to be known.

The dynamic zero shear viscosity $\eta_0(t)$ is varying with the material temperature T_m following an Arrhenius law:

$$\eta_0(t) = \eta_0 e^{(-bT_m)} \tag{10}$$

E. Boundary Conditions

Boundary conditions are expressed at the device inlet and outlet as well as at the edge between the partially and completely filled zones. Indeed, the model structures, according to the filling ratio between these two zones, are different. The system can therefore be decomposed into two subsystems, for which boundary conditions are expressed.

$$z = 0 : f = f_0; P = P_0; C = C_{in} \tag{11}$$

$$z = l_{pc} : f = f_{pc}; P = P_0; C = C_{pc} \tag{12}$$

$$z = L : f = 1; P = P_{end}; \frac{\partial C}{\partial z} = 0 \tag{13}$$

The index pc corresponds to the boundary between the partially and completely filled zones. L is the extruder length.

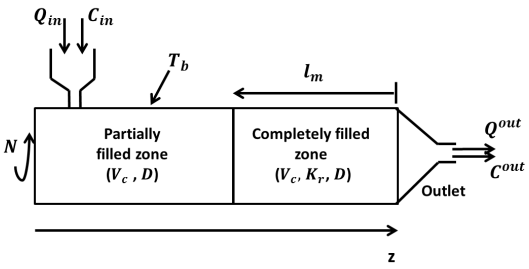

Fig. 2. Description of model parameters

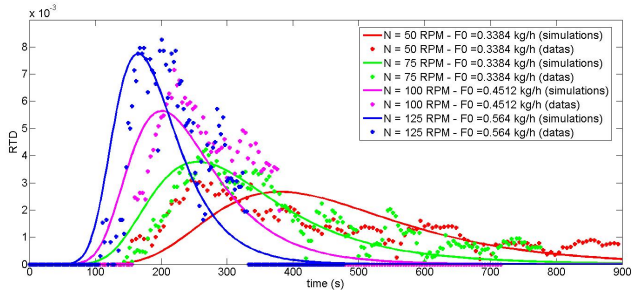

Fig. 3. Comparisons between the measured and simulated residence time distributions (RTD).

III. Parameter identification and simulation of the dynamic model

A dynamic model is described by equations (1) to (13) containing several parameters. The different mass flows are formulated using geometrical parameters (V_c and K_r) as well as the diffusion coefficient D (considered constant along the device). These 3 model parameters are a priori unknown and their influence on the extruder is illustrated in Figure 2.

A. Residence time distribution (RTD)

Estimation of the unknown parameters is achieved by fitting the model prediction to experimental data from a pilot plant. Measurements of the residence time distribution (RTD) describe the time spent by material elements inside the device and provides informative data about conveying and mixing behaviors of the extruder. When the device reaches steady-state, a tracer pulse is applied at the inlet and its resulting outlet concentration is measured.

The RTD is expressed as a normalization of this tracer concentration evolution as in:

$$E(t) = \frac{c(t)}{\int_0^{\inf} c(t)dt} \tag{14}$$

where $E(t)$ is the residence time distribution and $c(t)$ the tracer concentration evolution at the extruder output.

B. Expression of the cost function

Since measurement signals are corrupted by noise, parameter identification leads to uncertain estimates. Moreover, the model predictive capability can also be degraded by parameter variations following operating condition changes.

In this work, parameter identification is achieved while minimizing a simple least-squares cost function measuring the deviation between experimental data collected from the pilot plant and model state trajectories as in:

$$J(\theta) = \sum_{i=1}^{n_m \times n_e} \sum_{j=1}^{n_s} ((x_{ij}(\theta) - x_{meas,ij}(\theta))^T (x_{ij}(\theta) - x_{meas,ij}(\theta))) \tag{15}$$

where θ is the parameter vector, x_{ij} the j^{th} output state variable at time i and $x_{meas,ij}$ the corresponding experimental measurements. In equation (15), n_m measurements and n_e experiments are considered.

C. Selection of operating conditions

In order to collect sufficiently informative data, a wide experimental field is covered by four runs at different realistic operating points. These operating conditions are summarized in Table II.

D. Parameter identification

RTD experiments are achieved with a pilot extruder (located at the University of Liege (ULg)) running at different constant levels of rotation speed N (RPM) and feed rates F_0 $(kg/h$, h corresponds to hours, see Table II). Once the system reaches steady-state, a colorimetric test is used to determine the RTD (see [15]). During each experiment, an iron oxide pulse of 0.085 kg/h is applied at the inlet and the corresponding outlet concentration is measured every 4 s.

Four experiments are therefore performed and Table I shows the model parameter values and the absolute confidence intervals at 95% (based on the Fisher Information Matrix) resulting from the identification step. The optimizer $fminsearch$, using a Nelder-Mead algorithm [16] in the MATLAB environment, is used to perform the minimization of the cost function (15). This algorithm is robust to the presence of local minima, compared to gradient-based techniques.

Measured RTD fits quite well with model predictions as shown in Figure 3. Moreover, this qualitative statement is confirmed by the root mean-square error ($RMSE$), chosen as quantitative criterion (presented in Table II for each experiment) and expressed as:

$$RMSE = \sqrt{\frac{1}{n}\sum_{i=1}^{n}((x_{meas,i} - x_{model,i})^2} \tag{16}$$

where $x_{meas,i}$ and $x_{model,i}$ are respectively the i^{th} (over n) measured and modeled output state values.

TABLE I

Model parameter values

Model parameter	Identified value	Absolute confidence interval at 95%
$V_c(m^3)$	$4.2e^{-9}$	$0.3e^{-9}$
$K_r(m^4)$	$9.3e^{-11}$	$0.6e^{-11}$
$D(\frac{m^2}{s})$	$3.1e^{-5}$	$0.2e^{-5}$

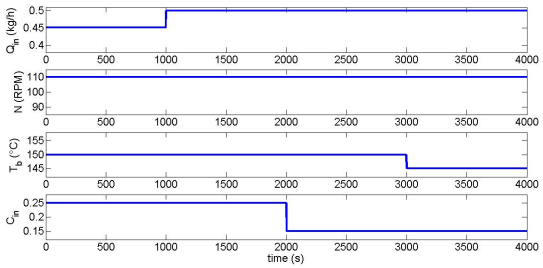

Fig. 4. Evolution of the input signals in simulation 1

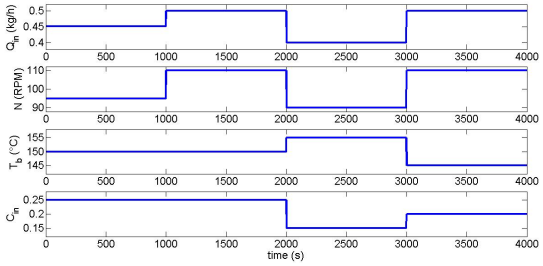

Fig. 5. Evolution of the input signals in simulation 2

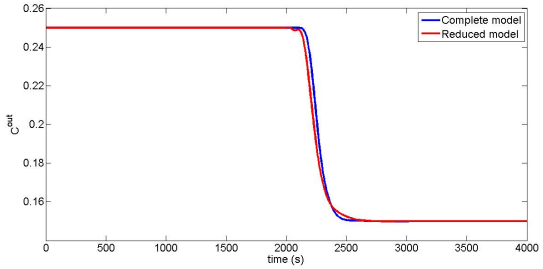

Fig. 6. Evolution of the output API concentration C^{out} in simulation 1

Figures 6, 7, 8 and 9 show the evolution of the output mass flow Q^{out} and the output API concentration C^{out} for each simulation.

TABLE II

OPERATING CONDITIONS AND RMSE FOR THE 4 RTD EXPERIMENTS

Run	N (RPM)	F_0 (kg/h)	RMSE
1	50	0.3384	$6.72e^{-4}$
2	75	0.3384	$6.04e^{-4}$
3	100	0.4512	$1.2e^{-3}$
4	125	0.564	$1.7e^{-3}$

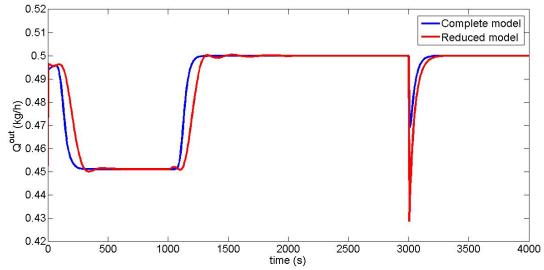

Fig. 7. Evolution of the output mass flow Q^{out} in simulation 1

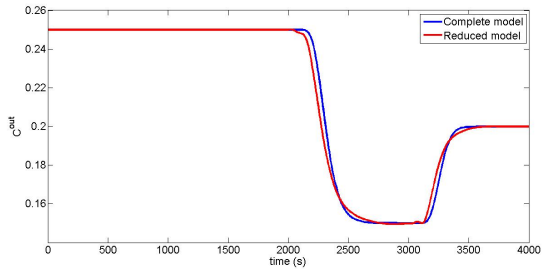

Fig. 8. Evolution of the output API concentration C^{out} in simulation 2

A good adequation between the two models is observed in Figures 6, 7, 8 and 9. For each input step, transient responses are relatively similar and values of the root mean-square errors (RMSE) are small for each simulation (see Table III). The main difference lies in the effect of the barrel temperature on the outflow Q^{out} which is larger in the "reduced model" than in the "complete model" (Figure 7). On the other hand, the computational cost for the simulation of the "complete model" is 15 times higher than for the "reduced model", which largely justifies the consideration of the latter in the control strategy.

TABLE III

RMSE BETWEEN THE "COMPLETE" AND THE "REDUCED" MODEL IN SIMULATIONS 1 AND 2

Output	RMSE (Simulation 1)	RMSE (Simulation 2)
C^{out}	0.0025	0.0028
Q^{out}	0.0057	0.0054

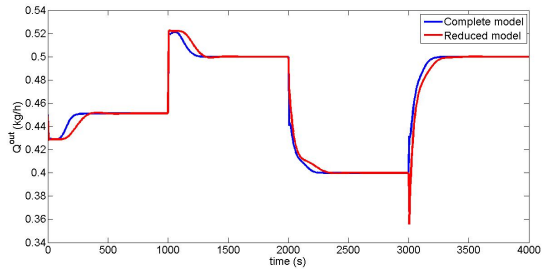

Fig. 9. Evolution of the output mass flow Q^{out} in simulation 2

E. Simulation study

In this section, predictions of the "complete" [11] and "reduced " ((1) to (13)) models are compared to assess the potential of the latter for the design of a model-based control strategy.

Two simulations are achieved with different input signals (see Figures 4 and 5). Initial operating conditions are $Q_{in} = 0.45\ kg/h$, $N = 100\ RPM$, $T_b = 150\ ^oC$ and $C_{in} = 0.25$.

Complex coupling between the inputs and outputs can also be considered. The output mass flow Q^{out} is mainly influenced by Q_{in} but important variations are also observed due to the rotation speed N and the barrel temperature T_b. These couplings would make the application of decentralized control strategies using, for instance, PID, delicate.

Two other aspects must also be taken into account in the solution of the control problem:

- the existence of a time delay (around 140 seconds for the chosen operating conditions), which is related to the particle circulation velocity inside the device;
- the presence of nonlinearities in the extrusion device (see [17]). In the current model, nonlinear phenomena are due to the evolution of the dynamic viscosity (equations (9) and (10)) and the presence of two filled areas in the extruder (with a filling ratio reaching the maximum value $f = 1$).

IV. Application of NMPC

Analysis of the dynamic model in section III and in [18] show the presence of complex input-output couplings, of a time delay and the existence of nonlinearities.

Nonlinear model predictive control (NMPC) strategy is suitable for the current problem ([19]) and a design is proposed for the regulation of the outlet API concentration C^{out} and the outlet flow Q^{out} using the feed flow rates Q_{in}, the screw rotation speed N, the barrel temperature T_b and the inlet API concentration C_{in}.

The control strategy is formulated as a constrained optimization problem where a cost function based on a quadratic error criterion representing the distance between the output predictions from the dynamic model and a reference trajectory is minimized. This optimization problem enables the determination of a control sequence over a horizon N_C based on model predictions (using system states x, outputs y and control variables u) over a horizon N_P. The problem is expressed as follows:

$$\min_{\boldsymbol{u_{k+1},\ldots,k+N_C}} J(t_k) \tag{17a}$$

$$\text{s.t.} \quad \dot{x} = f(x, \frac{\partial x}{\partial z}, \frac{\partial^2 x}{\partial z^2}, u), y = Cx,\ t \in [t_k, t_{k+N_P}] \tag{17b}$$

$$u(t) = u(t_{k+j-1}),\ j = 1, \cdots, N_C \tag{17c}$$

$$\boldsymbol{x}_{\min} \leqslant \boldsymbol{x} \leqslant \boldsymbol{x}_{\max} \tag{17d}$$

$$\boldsymbol{u}_{\min} \leqslant \boldsymbol{u} \leqslant \boldsymbol{u}_{\max} \tag{17e}$$

where $J(t_k)$ is the cost function, y_p is the output predictions and y^{ref} is the reference trajectory. Penalizations λ for control changes Δu are also taken into account:

$$J(t_k) = \sum_{i=1}^{N_P} (y_p(k+i) - y^{ref}(k+i))^2 + \lambda \sum_{j=1}^{N_C} (\Delta u_{k+j})^2 \tag{18}$$

At each time step, the minimization of the cost function (see equation (18)) is performed using the optimizer $fmincon$ from the MATLAB software. Physical constraint values and input penalizations are respectively shown in Table IV and V.

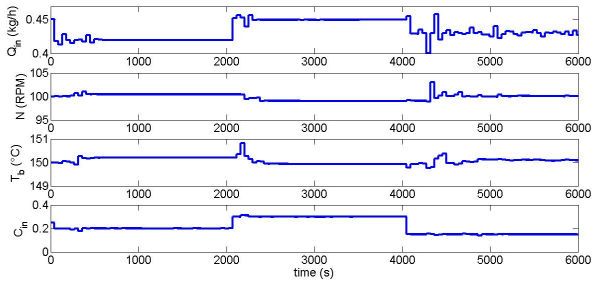

Fig. 10. Variation of the inputs Q_{in}, N, T_b and C_{in} in time with the NMPC control

TABLE IV

Input and output constraints

Variables	Minimum Values	Maximum Values
Inputs		
Q_{in}	0.35 kg/h	0.48 kg/h
N	90 RPM	110 RPM
T_b	145 ^oC	160 ^oC
C_{in}	0	0.5
Outputs		
Q^{out}	0.25 kg/h	0.5 kg/h
C^{out}	0.15	0.35

TABLE V

Δu penalizations

Input penalization	Values
Q_{in}	$\lambda_{Q_{in}} = 20$
N	$\lambda_N = 7e^{-6}$
T_b	$\lambda_{T_{b3}} = 0.031$
C_{in}	$\lambda_{C_{in}} = 0.032$

Simulation of the NMPC control is divided into different phases. In fact, setpoints vary with time t and model discrepancy and measurement noises are added during the simulation to analyze the robustness of the control strategy. Introduction of these two disturbances is summarized as follows:

- from $t = 0$ to $t = 2000$: Simulation without model discrepancy and measurement noises
- from $t = 2000$ to $t = 4000$: Simulation with parameter errors: 10% increase of the model parameter values from [11]. Simulation without measurement noise.
- from $t = 6000$ to $t = 8000$: Simulation without model discrepancy. Simulation with measurement noise, application of withe noise with 5% relative standard deviation on the measurements.

The good qualitative results illustrated in Figures 10 and 11 and the small root mean-square error (RMSE) values between control outputs and set points (for Q^{out}: $RMSE = 0.007$; for C^{out}: $RMSE = 0.048$) during simulations, using a sample time of 45 seconds and horizons $N_C = 3$ and $N_P =$

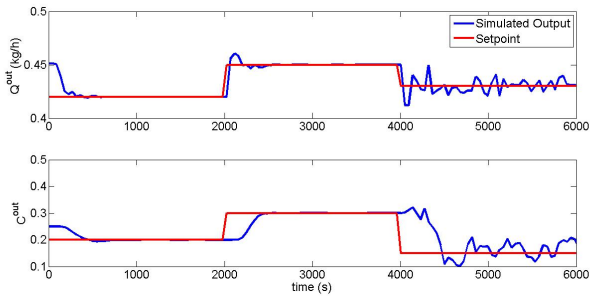

Fig. 11. Variation of the outputs Q^{out} and C^{out} in time with the NMPC control

6, show that the problem can be solved while respecting the constraints. Without any errors and noises, the setpoint tracking is very satisfactorily achieved. Introduction of model discrepancy does not deteriorate performance significantly. When measurement noise is present, control results are still quite good for Q^{out} but C^{out} seems more sensitive. The noise involves disturbances to the initial conditions in the prediction step and the result analysis shows a greater impact on the output API concentration C^{out} than the output flow Q^{out}. Moreover, simulation time for each control step is always smaller than the sampling time. The maximum simulation time is 85% of the sampling time (computation with a computer having a Dual-Core $i5$ (processor of $1.6\ GHz$)), which makes this computing time issue not critical (control is practically achievable) even if potentially improvable.

V. Conclusion

This paper presents a dynamic model and a mode-based control design for a pilot-plant extrusion device. A distributed parameter model based on partial derivative equations based only on mass balances, and a description of material rheology using the Yasuda-Carreau law, is formulated to predict the evolution of the output mass flow and the active pharmaceutical ingredient concentration. This "reduced model" has the advantage of being well-adapted to the design of a control strategy. An identification procedure using residence time distribution measurements is proposed to determine geometrical parameters and the diffusion coefficient. Good results obtained in this identification step and the realistic dynamic responses to step input variations confirm the ability of the model to predict the behavior of a real pilot plant extruder. Moreover, considering the existence of complex input-output couplings, of a time delay and nonlinearities, a NMPC formulation is proposed. Based on the solution of an input/output constrained optimization problem, this control strategy enables the regulation of the output concentration and the output flow while other physical variables are forced to respect some security thresholds (typical in pharmaceuticals) and mechanical/physical limitations. In the perspective of future experimental validations, model discrepancy and measurement noises are added to the simulations and the results demonstrate the robustness of the controller.

ACKNOWLEDGMENT

This paper presents research results of the Belgian Network DYSCO (Dynamical Systems, Control, and Optimization), funded by the Interuniversity Attraction Poles Programme, initiated by the Belgian State, Science Policy Office. The authors acknowledge the support of the WBgreen MYCOMELT project, achieved in collaboration with the University of Liege (ULg). The scientific responsibility rests with its author(s).

References

[1] H. Gerrens. *Handbuch der Technischen Polymerchemie.* Von A Echte. VCH Verlagsgesellschaft mbH,Weinheim. Chem. Ing. Tech. Volume 66, 239, 1994

[2] J. Hughey, J. Keen, D. Miller, K. Kolter, N. Langley and J. McGinity. *The use of inorganic salts to improve the dissolution characteristics of tablets containing Soluplus®-based solid dispersions* European Journal of Pharmaceutical Sciences, Elsevier, Volume 48, Number 4, pages 758-766, 2013

[3] J. Thiry, F. Krier and B. Evrard. *A review of pharmaceutical extrusion: Critical process parameters and scaling-up* International journal of pharmaceutics, Elsevier, Volume 479, Number 1, pages 227-240, 2015

[4] C. Abeykoon. *Single screw extrusion control: A comprehensive review and directions for improvements* Control Engineering Practice, Elsevier, Volume 51, pages 69-80, 2016

[5] B. Singh and S. Mulvaney. *Modeling and process control of twin-screw cooking food extruders* Journal of Food engineering, Elsevier, Volume 23, Number 4, pages 403-428, 1994

[6] J. Schlosburg. *Twin-Screw Food Extrusion: Control Case Study* 2005

[7] L. Wang, S. Smith and C. Chessari. *Continuous-time model predictive control of food extruder* Control Engineering Practice, Elsevier, Volume 16, Number 10, pages 1173-1183, 2008

[8] M. Trifkovic, M. Sheikhzadeh, K. Choo, K and S. Rohani. *Model predictive control of a twin-screw extruder for thermoplastic vulcanizate (TPV) applications* Computers & Chemical Engineering, Elsevier, Volume 36, pages 247-254, 2012

[9] P. Zhou, H. Liu, K. Tan and C. Chen. *Application and Research of Fuzzy Control Simulation in Twin Screw Extruder* Procedia Engineering, Elsevier, Volume 29, pages 542-546, 2012

[10] M.K. Kulshreshtha, C. Zaror. *An unsteady state model for twin screw extruders.* Food and Bioproducts Processing Volume 70, pages 21-28, 1992

[11] J. Grimard, L. Dewasme, A Vande Wouver. *Modeling, sensitivity analysis and parameter identification of a twin screw extruder.* IFAC-PapersOnLine, Volume 49, Number 7, pages 1127-1132, 2016

[12] M. Booy. *Isothermal flow of viscous liquid in corotating twin screw devices*. Polymer Engineering and Sciences, Vol. 20, 1980

[13] S. Choulak, F. Couenne, Y. Le Gorrec, C. Jallut, P. Cassagnau, A. Michel *Generic dynamic model for simulation and control of reactive extrusion*, Ind. Eng. Chem. Res., 43 (2004), p. 7373-7382

[14] O.S. Carneiro, J.A. Covas, B. Vergnes. *Experimental and theoretical study of twin-screw extrusion of Polypropylene.* Journal of Applied Polymer Sciences. Vol. 78, p. 1419-1430, 2000

[15] A. Kumar, G.M. Ganiyal, D.D. Jones., M.A. Hanna *Digital image processin for measurement of residence time distribution in a labatory extruder* Journal of Food Engineering, Vol. 75, p. 235244, 2006

[16] F. Gao, L. Han.*Implementing the Nelder-Mead simplex algorithm with adaptive parameter*. Computational Optimization and Application, Springer, 2012

[17] N. Cayot, D. Bounie and H. Baussart. *Dynamic modelling for a twin screw food extruder: Analysis of the dynamic behaviour through process variables*. Journal of food engineering, Vol 25, Number 2, pages 245-260, Elsevier, 1995

[18] J. Grimard, L. Dewasme and A. Vande Wouwer. *Nonlinear model predictive control of a twin-screw extruder*. System Theory, Control and Computing (ICSTCC),20th International Conference, IEEE,204-209, 2016

[19] L. Grüne and J. Pannek. *Nonlinear model predictive control*. Springer, 2011